Available online at www.sciencedirect.com
SCIENCE DIRECT®
Solar Energy 74 (2003) 489–495
SOLAR ENERGY

Performance of low bandgap thermophotovoltaic cells in a small cogeneration system

K. Qiu*, A.C.S. Hayden

CANMET Energy Technology Centre—Ottawa, Natural Resources Canada, 1 Haanel Drive, Ottawa, Ontario, Canada K1A 1 M1

Received 22 April 2003; received in revised form 27 May 2003; accepted 27 May 2003

Abstract

In recent years there has been significant progress in fabrication of low bandgap thermophotovoltaic (TPV) devices, such as InGaAsSb, InGaAs and GaSb cells. However, only limited data are available in the literature with respect to the performance of these TPV cells in combustion-driven radiant sources. In this study, power generation using InGaAsSb TPV cells has been investigated in a gas-fired home heating furnace. The radiant power density and radiant efficiency of a gas-heated radiator were determined at different degrees of exhaust heat recuperation. Heat recuperation is shown to have a certain effect on combustion operation and radiant power output. The electric output characteristics of the InGaAsSb TPV devices were investigated under various operating conditions. An electric power density of 5.4×10^{3} W m^{-2} was produced at a radiator temperature of 1463 K for the small cogeneration system. The cell short circuit density was observed to be greater than 1×10^{4} A m^{-2} at a radiator temperature of 1203 K. Furthermore, the design aspects of combustion-driven TPV systems have been discussed. It is shown that development of a special combustion device with high conversion level of fuel chemical energy to useful radiant energy is required, to improve further the system efficiency.

1. Introduction

Thermophotovoltaic (TPV) cells convert radiation energy directly into electricity. As contrasted with solar photovoltaics, TPV cells are illuminated by combustion-driven radiant sources. Since the radiant power density of these radiant sources can be made much greater than that of the sun, the electric power density of the TPV cells is much higher than that of solar cells. By means of a converter consisting of the TPV cells, power generation can be achieved in gas-fired residential heating appliances, forming cogeneration systems. Such integrated TPV appliances operate without connection to electric utility and excess power can be fed into home grid to supply other appliances, or supply electricity for external consumers. These TPV systems are particularly suited to small-scale cogeneration of power and heat as well as decentralized power production. Also, TPV generation of electricity has the potential application in portable generators, hybrid electric vehicles, recovery systems of high temperature waste heat from industrial processes, etc. In TPV power generation systems, combustion-driven radiant sources are utilized. The photons emitted from the sources at a temperature of practical interest are distributed at much lower energies or longer wavelengths in comparison to solar radiation. Thus, low bandgap (e.g., $E_g<0.75$ eV) TPV cells are usually used in the TPV systems to optimize the power density and efficiency. GaSb, InGaAsSb and InGaAs cells are three types of low bandgap TPV devices that presently are of considerable interest. Fraas et al. (1998;2002) explored the integration of GaSb TPV cells with a gas-fired space heater and radiant tube burner for use in combined heat and power systems. Horne et al. (2002) reported on developing a diesel-fired TPV portable generator using GaSb cells. As for InGaAsSb and InGaAs TPV devices, their diode behavior and electric characteristics have been reported and related mechanisms studied extensively (Sulima et al., 2000; Wojtczuk et al., 1998; Wang et al., 1998). Sulima et al. (2000) explored the effect of various Zn diffusion profiles in InGaAsSb cells with diffused emitters on the cell electric output characteristics. They noted that strong built-in electric fields near the

*Corresponding author. Tel.: +1-613-996-9516; fax: +1-613-992-9335.

E-mail address: kqiu@nrcan.gc.ca (K. Qiu).

0038-092X/03/$ – see front matter
doi:10.1016/S0038-092X(03)00194-4

Nomenclature

A_r	Radiator area (m^2)
ΔH_L	Fuel lower heating value (J kg^{-1})
m_{fuel}	Fuel mass flow rate (kg s^{-1})
p_{el}	Cell power density (W m^{-2})
P_{el}	Electric output power (W)
p_{rad}	Net radiant power density (W m^{-2})
Q_{chem}	Chemical energy input rate (W)
T_0	Ambient temperature (K)
$T_{ex,in}$	Exhaust gas temperature before entering recuperator (K)
T_{in}	Preheated air temperature (K)
ε	Relative air preheating
η_{cell}	Cell efficiency
η_{rad}	Radiant efficiency
η_{spe}	Spectral efficiency
η_{TPV}	Electric efficiency of TPV system

surface lead to a reduction of the saturation value of the injection component of dark current and hence to an increase in open circuit voltage. Wojtczuk et al. (1998) discussed the performance status of 0.55 eV InGaAs TPV cells, with the cells illuminated by electric light. Wang et al. (1998) reported on the growth, material characterization and device performance of lattice-matched InGaAsSb/GaSb TPV devices with cutoff wavelength extended from 2.3 to 2.5 μm. In these investigations, the methods of epitaxial growth include organo-metallic vapor phase epitaxy, molecular beam epitaxy and liquid phase epitaxy. In contrast to the considerable work carried out on TPV cell fabrication and mechanism investigations, only limited data are available in the literature with respect to the performance of these TPV cells in combustion-driven radiant sources or practical TPV cogeneration units. In order to provide the basis for the design of TPV power generation systems, it is necessary to study the performance of these TPV cells in combustion-driven radiant sources, specifically in gas-fired furnaces.

In the research presented below, power generation using InGaAsSb TPV cells was investigated in a gas-fired heating furnace. The electric output characteristics of the InGaAsSb TPV cells were examined under various combustion conditions. The combustion operation of the burner/radiator was also studied. Moreover, thermal energy flow over the TPV unit was analyzed, in order to elucidate the design aspects of TPV systems.

2. Experimental

The low bandgap TPV cells used in this study are quaternary semiconductor InGaAsSb cells (AstroPower, USA). Currently, mainly two designs of InGaAsSb cells are being developed. One involves a thick (3–5 μm) low-doped epitaxial p-emitter with an AlGaAsSb window layer. The other design involves a relatively thin (<0.7 μm) high-doped emitter without a window layer. The InGaAsSb cells used in this study were fabricated from the latter design. The cell size is 0.4×10^{-2} m in diameter. At 300 K, the nominal bandgap of the cells is 0.53 eV, which corresponds to a cutoff wavelength of 2.4 μm. The spectral response of the InGaAsSb cells has been investigated extensively by Sulima et al. (2000). Note that large InGaAsSb TPV cell module is not commercially available now and related studies are still underway. Nonetheless, it is technologically achievable and will be economically achievable if the module can be produced in quantity in the future.

The system testing was performed in an experimental set-up of a gas-fired heating furnace, shown in Fig. 1. The experimental cogeneration system consisted of a gas burner, a thermal radiator, a spectral control filter, TPV cells, a cooling device, an air recuperator. The set-up was equipped with various measuring devices and a data acquisition system. The gas-fired burner in the furnace is fully aerated, where gas and combustion air are entirely premixed before entering the burner. The air recuperator developed in this work was made of stainless steel. The broadband radiator with reticulated structure was made of SiC, having an emissivity of approximately 0.9. The spectral control filter in the experimental assembly has a high transmission (approximately 0.85) below the cutoff wavelength of InGaAsSb cells and a relatively high reflectivity (0.6–0.9) above 2.5 μm. Apparently, the filter is not ideal and still transmits a certain amount of non-convertible radiation energy. The radiant power output from the radiator was measured by means of a radiometer (Land 2π Ellipsoidal Radiometer, Land Combustion Limited, UK). The radiometer detects the radiant heat flux incident from a solid angle of 2π. This radiometer is sensible to broadband radiation. The radiant efficiency is calculated from (Qiu and Hayden, 2003; Qiu et al., 2003):

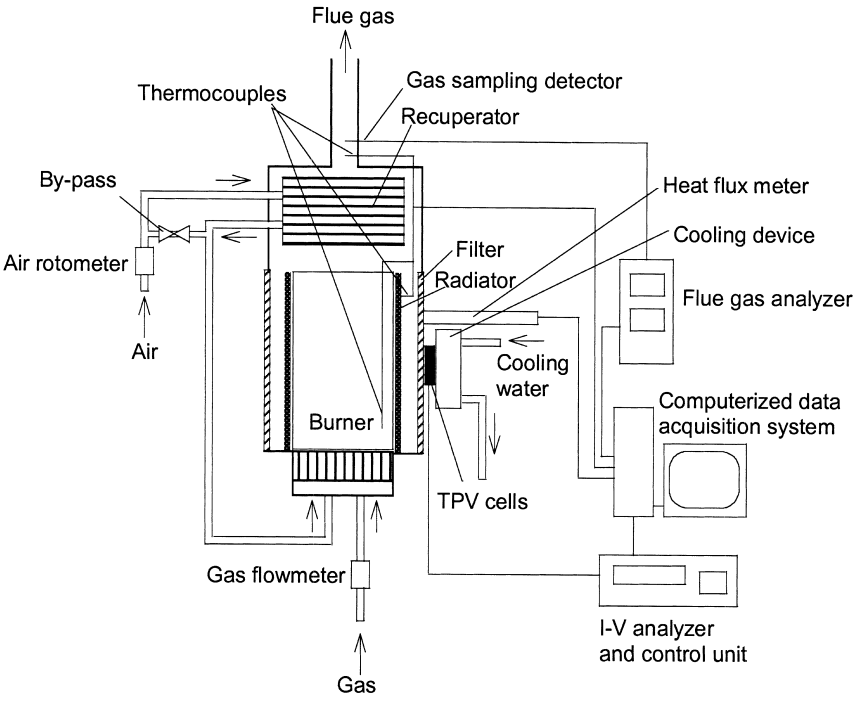

Fig. 1. Schematic diagram of the TPV experimental set-up.

$$\eta_{\mathrm{rad}} = \frac{p_{\mathrm{rad}} A_{\mathrm{r}}}{m_{\mathrm{fuel}} \Delta H_{\mathrm{L}}} \tag{1}$$

where p_{rad} is the net radiant power density, A_{r} is the radiator area, m_{fuel} is the fuel mass flow rate and ΔH_{L} is the fuel lower heating value. The net radiant power refers to the amount of radiation transmitted by the filter. The fuel flow rate into the burner was obtained from a gas flowmeter, thus enabling the determination of heat input rate. In order to examine the effect of firing rate on radiation behavior at predetermined excess air, the air and fuel flow rates were changed simultaneously. Thermocouples were used to measure the temperatures of flue gas and radiator. Five thermocouples were installed on the radiator. The thermocouple tips were cemented on the surface of the radiator. It should be noted that there were some uncertainties and factors that may affect the accuracy of the radiator temperature measurements (although corrected for heat transfer effects on thermocouple tips). The temperature of preheated air was also measured using thermocouples. Flue gas composition (O_2, CO_2, CO and NO_x) was monitored with paramagnetic, infrared-chemiluminescent flue gas analyzers (Qiu and Hayden, 2003).

3. Experimental results

Table 1 shows the major results of combustion operation of the experimental set-up. The radiant power density and radiant efficiency of the gas-heated radiator were determined at varying degrees of exhaust heat recuperation or

Table 1
Results of combustion performance of the experimental set-up

Heat release rate[a] (W)	Relative air preheating	Air temperature (K)	Radiator temperature (K)	Net radiant power density (W m^{-2})	Radiant efficiency (%)
4.8×10^3	0	297	1203	3.5×10^4	21.7
5.5×10^3	0	297	1243	3.9×10^4	21.1
6.3×10^3	0	297	1278	4.4×10^4	20.7
6.9×10^3	0	297	1323	4.7×10^4	20.6
6.9×10^3	0.18	538	1404	5.6×10^4	24.1
6.9×10^3	0.31	745	1463	6.1×10^4	26.3

[a] Fuel: Natural gas.

relative air preheating. The relative air preheating, ε, is defined as:

$$\varepsilon = \frac{T_{in} - T_0}{T_{ex,in} - T_0} \quad (2)$$

where T_{in} is the preheated air temperature, T_0 is the ambient temperature and $T_{ex,in}$ is the exhaust gas temperature before entering recuperator. The heat recuperation was observed to have a significant influence on the combustion operation and radiant power output. In general, however, the radiation source efficiency achieved in the combustion unit is modest (Table 1). This is ascribed mainly to the relatively low radiator temperature and also to the fact that the burner/radiator used in this work was not designed for maximization of radiant efficiency. In a previous paper (Qiu and Hayden, 2003), it has been shown that the reticulated (honeycomb-like) radiator geometry and combustion mode affect on the radiator temperature and the radiant efficiency.

The electric output characteristics of the InGaAsSb TPV cells were measured, with the cells illuminated by the gas-heated radiator in the furnace under various operating conditions. Fig. 2 shows the variations of open circuit voltage with short circuit current density at different cell temperatures. At a low cell temperature (approximately 297 K), the open circuit voltage increases with short circuit current density as the radiator temperature or radiant power density is raised. At a given radiation intensity, the short circuit current and open circuit voltage are affected by the Zn concentration profile in p-$In_{0.15}Ga_{0.85}As_{0.17}Sb_{0.83}$ emitter (Sulima et al., 2000). The surface treatment and front contact fabrication also have an influence on the short circuit current. Superior light trapping and/or higher absorption coefficients enhance the short circuit current density.

The results presented in Fig. 2 indicate that the open circuit voltage is higher than 0.3 V at a short circuit current density greater than 1×10^4 A m^{-2}. Interestingly, the dependence of open circuit voltage on the circuit density was altered when the cell temperature was elevated. Note that the filtered radiation contained a certain amount of non-convertible radiation energy. This energy became waste heat when it was incident on the cells. Although the waste heat was dissipated with the water-cooled heat sink, it was found that a certain rise in the cell temperature appeared to be inevitable after the cells had been exposed to the radiant source in the furnace for some time. It is known that for the very low bandgap InGaAsSb cells, the cell temperature greatly influences the open circuit voltage, especially under high current density conditions. For instance, in the range 297 to 333 K, the temperature coefficient of open circuit voltage was reported ranging from -1.79×10^{-3} to -43×10^{-3} V K^{-1} at current densities of 0.3–6.0×10^4 A m^{-2} (Sulima et al., 2000). In consequence, the open circuit voltage decreased with short circuit current density at elevated cell temperatures in the system testing. This is apparently ascribed to a greater temperature coefficient of open circuit voltage at a higher current density. Fig. 3 presents the short circuit current density and open circuit voltage as a function of radiator temperature at different cell temperatures.

Fig. 4 shows the measured power density as a function of radiator temperature during the system testing. As

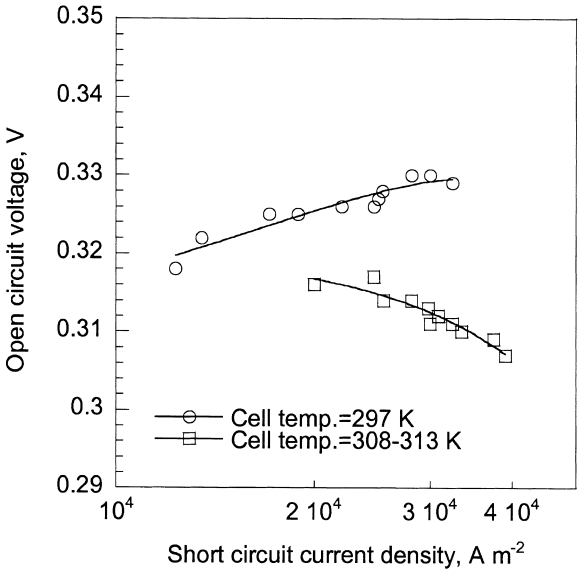

Fig. 2. Variations of open circuit voltage with short circuit current density at different cell temperatures in the system testing.

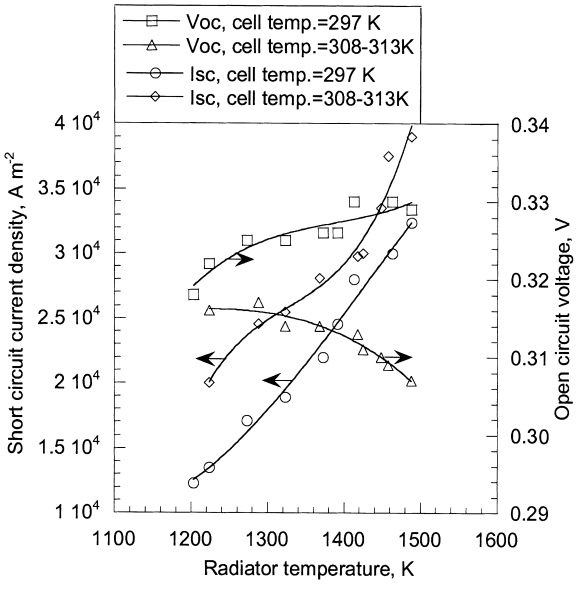

Fig. 3. Short circuit current density and open circuit voltage as a function of radiator temperature at different cell temperatures.

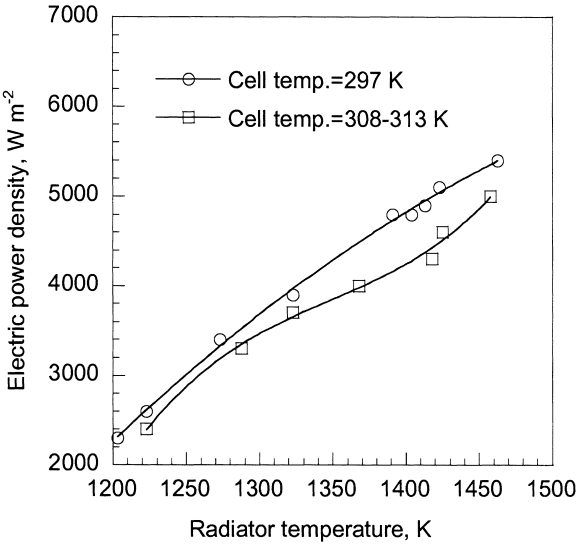

Fig. 4. Electric power out density vs. radiator temperature at different cell temperatures.

expected, the power output noticeably increases with the radiator temperature. Obviously, the cell temperature has an influence on the maximum power output. On the one hand, increasing cell temperature gives rise to a reduction in open circuit voltage (Fig. 3) as well as fill factor. On the other hand, the cell spectral response increases with rising cell temperature, thereby resulting in a significant rise in the current density (Fig. 3). As a consequence of these combined effects, the electric power density drops off only slightly over the cell temperature range being considered. As shown in Fig. 4, a reasonably high power density has been produced by the low bandgap TPV cells in the combustion-driven radiant source, despite a certain rise in the temperature of cells in the heating furnace.

4. Discussion

As noted earlier, the size of the cells tested in this research is 0.4×10^{-2} m in diameter. Therefore, they do not cover the whole radiator, but the maximum power generation can be projected from the obtained cell power density and the actual radiator area in the experimental set-up. Table 2 presents the results of electric power density and projected power output for the experimental TPV unit under various combustion conditions. It is seen that the modest air preheating results in a significant increase in the electric power output.

From the obtained experimental data and thermal energy flow over the TPV system, the system efficiency may be analyzed. The components of the experimental TPV unit and thermal energy flow over the system are schematically depicted in Fig. 5. The heat flux transferred from combustion products to the radiator is emitted. The radiation energy is subsequently filtered by the spectral control filter. The combustion products leaving the burner/radiator enter the air recuperator, by which part of the sensible heat of the products is transferred to combustion air. The combustion air is thus preheated from ambient temperature to a desirable temperature. The TPV devices convert the in-band radiation incident on them into electricity at specific cell efficiency. Finally, the exhaust gases leaving the recuperator enter a heat exchanger for space heating.

The electric efficiency of TPV system is defined as the ratio of electric output power, P_{el}, to chemical energy input rate, Q_{chem}:

$$\eta_{TPV} = \frac{P_{el}}{Q_{chem}} \tag{3}$$

or:

$$\eta_{TPV} = \frac{p_{el}A_r}{Q_{chem}} \tag{4}$$

where p_{el} is the cell power density. Conceptually, TPV generation systems seem quite simple. However, the development of these systems has proved to be much more challenging than anticipated (Schroeder, 1998). During the process of TPV conversion, the three primary components, heat source/thermal radiator, spectral control filter and bandgap-matched TPV cells, must function as a well-integrated system. The system efficiency can also be

Table 2
Experimental data of electric power density and projected power output for the experimental TPV unit under various combustion conditions

Heat release rate (W)	Relative air preheating	Radiator temperature (K)	Cell electric power density[a] (W m^{-2})	Projected power output[b] (W)
4.8×10^3	0	1203	2.3×10^3	68.3
5.5×10^3	0	1243	2.8×10^3	83.2
6.3×10^3	0	1278	3.4×10^3	101.0
6.9×10^3	0	1323	3.9×10^3	115.8
6.9×10^3	0.18	1404	4.8×10^3	142.6
6.9×10^3	0.31	1463	5.4×10^3	160.4

[a] The cell power density was obtained at a cell temperature of approximately 297 K.
[b] Total cell area is assumed to amount to the radiator area (2.97×10^{-2} m^2).

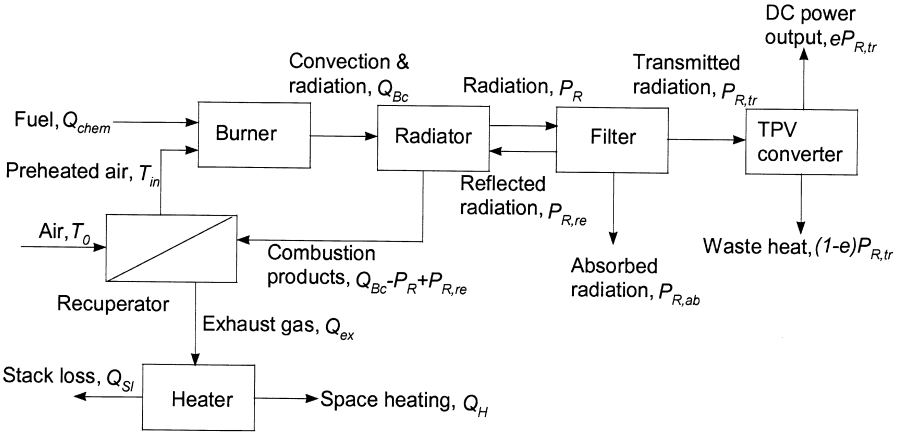

Fig. 5. Energy flow diagram for the combustion-driven TPV cogeneration system.

expressed as the product of efficiencies of the three components (see Fig. 5), i.e.:

$$\eta_{\mathrm{TPV}} = \eta_{\mathrm{rad}}\eta_{\mathrm{spe}}\eta_{\mathrm{cell}} \tag{5}$$

where η_{spe} is the spectral efficiency and η_{cell} is the cell efficiency. The spectral efficiency refers to the ratio of the radiant power output with TPV cell convertible wavelengths to the total net radiant power output. The cell efficiency is here defined as the ratio of maximum electric power to photon convertible radiant power. Note that Eq. (5) implies that all net radiation output is incident on the cells. The component efficiencies for the experimental system have been calculated and are given in Table 3. Since it was impossible to measure the cell efficiency precisely for the present experimental facility, the cell efficiency was estimated from the modeling calculations (Qiu et al., 2003).

As shown in Table 3, the major energy loss in the system results from the low conversion of fuel energy to photon convertible radiation. Therefore, in order to realize high-efficiency TPV systems and thus approach commercial readiness, further work should be directed to developing a special gas combustion device with a high conversion level of fuel chemical energy to useful radiant energy. For instance, it has been reported that a gas-fired self-recuperative SiC radiant-tube burner can operate at an outer tube surface temperature of 1523 K, with the temperature uniformity being within ±10 K (Wunning and Wunning, 1996). The thermal efficiency of the radiant-tube burner could reach the level of 70% when using a built-in ceramic recuperator with relative air preheating above 0.65 (e.g., air preheating temperature at 1118 K). The radiant tubes for higher temperatures are under development. Such radiant-tube burners may offer the potential for high system efficiency for TPV power production (Fraas et al., 2002). In addition, it has been known that the fuel-to-convertible radiation efficiency can be increased through the use of selective radiators such as tungsten radiator and antireflective material coated tungsten radiator (Gombert, 2002). However, these selective radiators are not without problems and they are still under study.

It should be noted that the TPV generation in gas-fired heating appliances is a cogeneration system where exhaust heat is in large part utilized for space and/or water heating. Hence, in spite of a relatively low system electric efficiency, the overall fuel utilization efficiency in such a system can be sufficiently high, e.g., higher than 90%. Also, for the cogeneration system, the required electricity share is usually small, as compared with the thermal load.

Table 3
Component efficiencies for the experimental TPV system

Heat release rate (W)	Radiator temperature (K)	Radiant efficiency (η_{rad}) (%)	Spectral efficiency (η_{spe}) (%)	Conversion of fuel to photon convertible radiation ($\eta_{\mathrm{rad}}\eta_{\mathrm{spe}}$) (%)	Cell efficiency (η_{cell}) (%)
4.8×10^3	1203	21.7	34.8	7.5	19.1
5.5×10^3	1243	21.1	37.0	7.8	19.4
6.3×10^3	1278	20.7	39.1	8.1	19.7
6.9×10^3	1323	20.6	40.8	8.4	20.0
6.9×10^3	1404	24.1	41.5	10.0	20.6
6.9×10^3	1463	26.3	42.2	11.1	20.9

Therefore, the simultaneous production of electric power and heat in residential homes using the TPV converter is still very attractive, even when the system electric efficiency is not very high. It is expected that with further optimization of cell structure and manufacturing process, and with enhancement of the thermal design of TPV cogeneration systems, a power density on the order of 1.0×10^4 W m^{-2} and a TPV electric system efficiency higher than 10% will be achieved in the near future. For the next step, a prototype of commercial-scale TPV cogeneration residential boiler will be developed in order to evaluate various issues related to this technology and thus try to approach commercial readiness. This will be of particular interest to off-grid homes and remote communities. Also, as indicated by other researchers (Fraas et al., 1998), the TPV units are complimentary to solar photovoltaic systems in cold climates and during the wintertime when the sun is not shining or the radiation density is too weak.

5. Conclusions

Performance of low bandgap InGaAsSb TPV cells was investigated in a gas-fired furnace where a thermal radiator was heated directly by a combustion flame. The radiant power and radiant efficiency were determined under various operating conditions. It has been shown that exhaust heat recuperation has a significant effect on the burner/radiator operation. The cell short circuit density was greater than 1×10^4 A m^{-2} at a relatively low radiator temperature of 1203 K. A power density of 5.4×10^3 W m^{-2} was reached at a radiator temperature of 1463 K. The obtained experimental results suggest that the simultaneous production of heat and electric power using TPV cells in residential homes is very attractive. The analyses of energy flow over the TPV unit showed that the major energy loss arose from the low conversion of fuel chemical energy to photon convertible radiation. Therefore, a gas burner/radiator system with a high conversion level of fuel energy to useful radiant energy is required for high-efficiency TPV units.

Acknowledgements

The authors would like to thank Dr. M.G. Mauk of AstroPower, Inc., USA, for his valuable help and discussions. Funding for this activity is primarily from the Canadian Program on Energy Research and Development (PERD).

References

Fraas, L., Avery, J., Malfa, E., Wuenning, J.G., Kovacik, G., Astle, C., 2002. Thermophotovoltaics for combined heat and power using low Nox gas fired radiant tube burners. In: Proceedings of the 5th Conference on Thermophotovoltaic Generation of Electricity, pp. 61–70.

Fraas, L., Ballantyne, R., Hui, S, Ye, S.Z., Gregory, S., Keyes, J., Avery, J., Lamson, D., Daniels, B., 1998. Commercial GaSb cell and circuit development for the midnight sun TPV stove. In: Proceedings of the 4th NREL Conference on Thermophotovoltaic Generation of Electricity, pp. 480–488.

Gombert, A., 2002. An overview of TPV emitter technology. In: Proceedings of the 5th Conference on Thermophotovoltaic Generation of Electricity, pp. 123–131.

Horne, W.E., Morgan, M.D., Sundaram, V.S., Butcher, T., 2002. 500 Watt diesel fueled TPV portable power supply. In: Proceedings of the 5th Conference on Thermophotovoltaic Generation of Electricity, pp. 91–100.

Qiu, K., Hayden, A.C.S., 2003. Thermophotovoltaic generation of electricity in a gas-fired heater: influence of radiant burner configurations and combustion processes. Energy Convers. Manage., in press.

Qiu, K., Hayden, A.C.S., Mauk, M.G., 2003. Generation of electricity using InGaAsSb and GaSb TPV cells in combustion-driven radiant sources. In progress.

Schroeder, K.L. (1998). Performance optimization of thermophotovoltaic systems. Ph.D. Thesis. Auburn University, Auburn, AL.

Sulima, O.V., Beckert, R., Bett, A.W., Cox, J.A., Mauk, M.G., 2000. InGaAsSb photovoltaic cells with enhanced open-circuit voltage. IEE Proc. Optoelectron. 147, 199–204.

Wang, C.A., Choi, H.K., Oakley, D.C., Charache, G.W., 1998. Extending the cutoff wavelength of lattice-matched GaInAsSb/GaSb thermophotovoltaic devices. In: Proceedings of the 4th NREL Conference on Thermophotovoltaic Generation of Electricity, pp. 256–265.

Wojtczuk, S., Colter, P., Charache, G., DePoy, D., 1998. Performance status of 0.55 eV InGaAs thermophotovoltaic cells. In: Proceedings of the 4th NREL Conference on Thermophotovoltaic Generation of Electricity, pp. 417–426.

Wunning, J.A., Wunning, J.G., 1996. Ceramic burner and radiant tubes for high-temperature processes. Tile Brick Int. 12 (5).